



Synthesis and NMR studies of the polymer membranes based on poly(4-vinylbenzylboronic acid) and phosphoric acid

Aslıhan Sezgin^a, Ümit Akbey^b, Michael Ryan Hansen^b, Robert Graf^b, Ayhan Bozkurt^{a,*}, Abdülhadi Baykal^a

^a Department of Chemistry, Fatih University, 34500 Büyükcçekmece–İstanbul, Turkey

^b Max-Planck-Institut für Polymer Research, Ackermannweg 10, D-55128 Mainz, Germany

ARTICLE INFO

Article history:

Received 18 April 2008

Received in revised form 3 July 2008

Accepted 3 July 2008

Available online 10 July 2008

Keywords:

Poly(4-vinylbenzylboronic acid)

Proton conductivity

NMR studies

ABSTRACT

Proton conduction in novel anhydrous membranes based on host polymer, poly(4-vinylbenzylboronic acid), (P4VBBA) and phosphoric acid, (H₃PO₄) as proton solvent was studied. The materials were prepared by the insertion of the proton solvent into P4VBBA at different stoichiometric ratios to get P4VBBA·xH₃PO₄ composite electrolytes. Homopolymer and the composite materials were characterized by FT-IR, ¹¹B MAS NMR and ³¹P MAS NMR. ¹¹B MAS NMR results suggested that acid doping favors or leads to a four-coordinated boron arrangement. ³¹P MAS NMR results illustrated the immobilization of phosphoric acid to the polymer through condensation with boron functional groups (B–O–P and/or B–O–P–O–B). Thermogravimetric analysis (TGA) showed that the condensation of composite materials starts approximately at 140 °C. An exponential weight loss above this temperature was attributed to intermolecular condensation of acidic units forming cross-linked polymer. The insertion of phosphoric acid into the matrix softened the materials shifting *T_g* to lower temperatures. The temperature dependence of the proton conductivity was modeled with Arrhenius relation. P4VBBA·2H₃PO₄ has a maximum proton conductivity of 0.0013 S/cm at RT and 0.005 S/cm at 80 °C.

© 2008 Elsevier Ltd. All rights reserved.

1. Introduction

The demand for proton conducting anhydrous membranes has been increased over the last decade due to their use in fuel cells, as well as in electrochromic displays, sensors and super capacitors [1–4]. Although there are several approaches for anhydrous systems, previous concept was mainly based on the doping of the polymers bearing basic sites with inorganic acids (e.g. H₃PO₄, H₂SO₄). Pure H₃PO₄ itself is a good proton conductor because of its extensive self-ionization and low *pK_a*. Structure diffusion was proposed as the proton transport mechanism in fused phosphoric acid, where the transference number of proton is close to unity (~0.975) [5]. Phosphoric acid interacts with polymers through hydrogen bonds and facilitates the formation of homogeneous blends. In general, phosphoric acid in polymer electrolytes acts as proton solvent and as well as plasticizer increasing the co-operative segmental motions of the polymer chains. Several homogeneous polymer electrolytes such as poly(ethylene-oxide)·xH₃PO₄ [6], poly(vinylalcohol)·xH₃PO₄ [7], linear (L) or

branched (B) polyethyleneimine·xH₃PO₄ [8,9], poly(acrylamide)·xH₃PO₄ [10], poly(vinylpyrrolidone)·xpolyphosphoric acid [11] were reported. In addition, extensive research on more stable systems such as phosphoric acid doped polybenzimidazole (PBI) has been done and physicochemical characterizations as well as fuel cell performances were reported [4,12–15].

In these polymer electrolytes the structural diffusion is predominant where the proton diffusion is mainly controlled by proton transport within non-aqueous phase, i.e., proton exchange between H₄PO₄⁺ and H₂PO₄⁺ [4]. In addition to these, heterogeneous systems based on phosphoric acid incorporated Nafion yielded a super acid under anhydrous conditions where the charged species are generated yielding excess H₄PO₄⁺ and an immobilized –SO₃[–] anion [16]. The self-ionization of the phosphoric acid is reduced, yielding a lower concentration of the H₂PO₄⁺ ion. Then the proton transport through structure diffusion is reduced. Different from Nafion/H₃PO₄ system, it would be useful to develop an alternative host matrix where the channels can be filled with phosphoric acid and diffusion can occur over the acidic phase. Moreover, the absence of strong acidic units in the host material such as –SO₃H may enhance the structure diffusion between H₄PO₄⁺ and H₂PO₄⁺.

To have such membranes, it would be interesting to use thermally stable boronic acid functional polymers such as

* Corresponding author. Tel.: +90 212 8663300; fax: +90 212 8663402.
E-mail address: bozkurt@fatih.edu.tr (A. Bozkurt).

poly(4-vinylbenzylboronic acid) as host matrix. The insertion of phosphoric acid may cause phosphoric acid functional polymers by forming a chemical linkage, i.e., B–O–P at higher temperatures. Previously it was reported that the homopolymers and copolymers with boron show higher thermal stability than homologous polymers without boron [17]. In addition, boronphosphate (BPO_4) was used as an important additive in sulfonated polymers, i.e., SPEEK which contributed positively to the mechanical properties as well as proton conductivity of the polymer electrolyte membranes [18,39]. An interesting feature of BPO_4 is that it retains water up to 300°C [19]. The adsorbed water is present in a partially dissociated form because the surface is also covered with hydroxyl groups of various types, i.e., free B–OH, P–OH, geminal P–OH and H-bonded OH groups associated with both B and P. BPO_4 acts as a proton conductor probably due to the presence of the above-mentioned protogenic groups on the surface [20]. The conductivity of BPO_4 increased with atomic ratio of B/P and reached to a maximum value when B/P ratio is 0.80 [21].

This paper reports on a new host matrix, poly(4-vinylbenzylboronic acid), P4VBBA which was produced by free radical solution polymerization of 4-vinylbenzylboronic acid (Fig. 1). Then P4VBBA was doped with phosphoric acid at several stoichiometric ratios. The membranes' properties were investigated by FT-IR, ^{11}B MAS NMR, ^{31}P MAS NMR, TG and DSC. The proton conductivity of anhydrous electrolytes was measured with a dielectric-impedance analyzer.

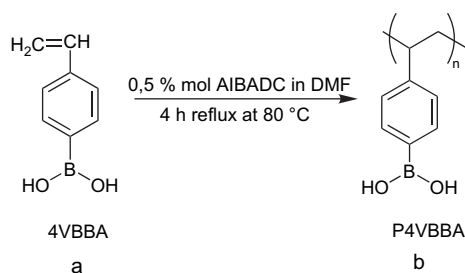


Fig. 1. Synthesis scheme of P4VBBA.

2. Experimental

2.1. Materials

4-Vinylbenzeneboronic acid (>98%) was provided from Alfa Aesar. The initiator α,α' -Azodiisobutyramidin dihydrochloride (AIBADC) was supplied from Aldrich. Orthophosphoric acid (>99%) and DMF were purchased from Merck.

2.2. Sample preparation

Poly(4-vinylbenzeneboronic acid), P4VBBA, was produced by free radical polymerization of 4-vinylbenzeneboronic acid in DMF using AIBADC (0.5 mol %). The reaction mixture was purged with nitrogen and the polymerization reaction was performed at 70°C for 4 h (Fig. 1). After polymerization of 4VBBA in DMF, the resulting solid was filtered and washed several times with excess DMF. The gel materials were cast onto polished Teflon plates and after drying under vacuum, transparent films with a thickness of about $200\ \mu\text{m}$ were obtained. Doping of the polymers was performed at different stoichiometric ratios, x , by swelling of the polymer in concentrated solution of phosphoric acid in DMF. The materials with $x = 1$ and $x = 2$ were prepared and they were dried under vacuum and stored in the glove box.

2.3. Characterizations

Fourier Transform infrared (FT-IR) spectra of the samples were scanned in the transmission mode using a Mattson Genesis II spectrophotometer.

Thermogravimetric analyses (TGA) of the composite electrolytes were carried out using Perkin-Elmer Pyris I instrument. The samples ($\sim 10\ \text{mg}$) were heated from room temperature to 750°C under inert atmosphere at a scanning rate of $10^\circ\text{C}/\text{min}$.

Netsch Differential Scanning Calorimeter DSC 404C Pegasus was used for DSC analysis. The measurements were carried out under nitrogen atmosphere at a rate of $10^\circ\text{C}/\text{min}$ and second heating curves were evaluated.

The proton conductivity of the composite electrolytes was measured using a Novocontrol dielectric-impedance analyzer. The materials were placed between two platinum electrodes and the proton conductivities were measured from 1 Hz to 3 MHz at several temperatures. The DC conductivities were derived from the plateaus of the AC conductivity data.

The ^{11}B 3Q-MAS experiments were performed on a Bruker DSX spectrometer at a boron Larmor frequency of 160.46 MHz and at room temperature with 20 kHz MAS. The three-pulse sequence with a z-filter [16,22] ^1H decoupling during acquisition was used to perform the experiments. The 90° pulse lengths were $2.5\ \mu\text{s}$ for both ^1H and ^{11}B (100 kHz rf nutation frequency). The optimized pulse lengths for the 3Q-MAS experiment were $5\ \mu\text{s}$ for P1 pulse (excitation, hard pulse), $2\ \mu\text{s}$ for P2 pulse (reconversion/mixing, hard pulse), and $10\ \mu\text{s}$ for P3 pulse (read out, soft pulse).

The ^{31}P MAS experiments were performed on a Bruker DSX spectrometer at a phosphorous Larmor frequency of 202.46 MHz at room temperature under 20 kHz MAS. The 90° pulse lengths were $2.5\ \mu\text{s}$ for both channels ^1H and ^{31}P , which correspond to 100 kHz radio-frequency nutation frequency.

3. Results and discussions

3.1. FT-IR study

The FT-IR spectra of homopolymer P4VBBA and acid doped P4VBBA $\cdot x\text{H}_3\text{PO}_4$ are shown in Fig. 2. The OH stretching of $-\text{B}(\text{OH})_2$ group gives a broad peak at around $3380\ \text{cm}^{-1}$. The aromatic CH stretching is located at $3030\ \text{cm}^{-1}$ and the absorption bands at $2930\ \text{cm}^{-1}$ and $2850\ \text{cm}^{-1}$ are assigned to the symmetric and antisymmetric stretching vibrations of aliphatic CH units. Two

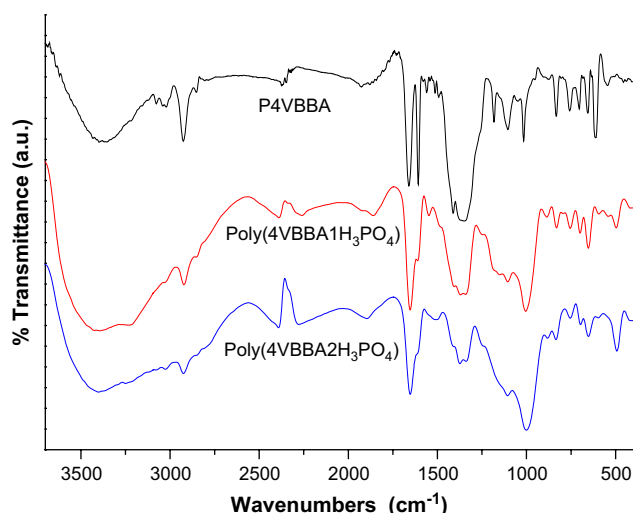


Fig. 2. FT-IR spectra of pure P4VBBA and doped P4VBBA $\cdot x\text{H}_3\text{PO}_4$ for $x = 1$ and $x = 2$ ratios.

strong peaks at 1660 cm^{-1} and 1606 cm^{-1} are attributed to C=C stretching bands of *p*-disubstituted benzene ring. The strong CH out-of plane deformation band for *p*-disubstituted benzene ring is at 835 cm^{-1} . The vibration of phenyl boronic acid linkage (Ph-B) gives a strong peak at 1420 cm^{-1} . The absorption bands at 1342 cm^{-1} and 1105 cm^{-1} are assigned to the vibrations of the bonds B–O and B–OH. The OH deformation of $-\text{B}(\text{OH})_2$ group is located at 1006 cm^{-1} [23]. Other important absorption signal near 760 cm^{-1} corresponds to B–O–B stretching vibration due to the cross-linked boronic acid units [24]. The absorption bands at 655 cm^{-1} and 615 cm^{-1} are assigned to out-of plane –OH bending [25]. After doping P4VBBA with H_3PO_4 , the broad and strong peaks appear near 1000 cm^{-1} which are attributed to PO_2 bending vibration and P–OH symmetric stretching of H_3PO_4 [26]. The intensity of the peak at 1342 cm^{-1} decreased due to possible intramolecular condensation of B–OH forming B–O–B linkages and also intermolecular condensation of B–OH and P–OH forming B–O–P bonds. Additionally, it was previously reported that the characteristic B–O–P band should appear near 1000 cm^{-1} [27,28]. However, the presence of P–O–H strong stretching within this region masked possible B–O–P stretching vibration within this domain [28].

3.2. Thermal analysis

The TGA results of the homopolymer and polymer electrolytes are illustrated in Fig. 3. For P4VBBA, the exponential weight decay up to approximately $400\text{ }^\circ\text{C}$ can be attributed to condensation of B–OH units then the polymer decomposes. The thermal stability of the composite electrolytes well improved after doping with H_3PO_4 i.e., the host polymer becomes stable up to $140\text{ }^\circ\text{C}$. The composite electrolytes represent an exponential weight change within $160\text{--}350\text{ }^\circ\text{C}$ due to intermolecular condensation of the acidic units. Weight loss above $350\text{ }^\circ\text{C}$ can be attributed to water liberation due to the self-condensation of the phosphoric acid as well as the decomposition of the polymer.

Fig. 4 shows the DSC thermograms of P4VBBA and phosphoric acid doped samples, $\text{P4VBBA} \cdot x\text{H}_3\text{PO}_4$. No distinct glass transition was observed for the host polymer, P4VBBA within the temperature range of measurement. However, as the phosphoric acid mole ratio increases in homopolymer, T_g shifts to lower temperatures. The glass transition temperature, $T_g = 95\text{ }^\circ\text{C}$ for $x = 1$ and $T_g = -8\text{ }^\circ\text{C}$ for $x = 2$. These results show the softening effect of phosphoric acid.

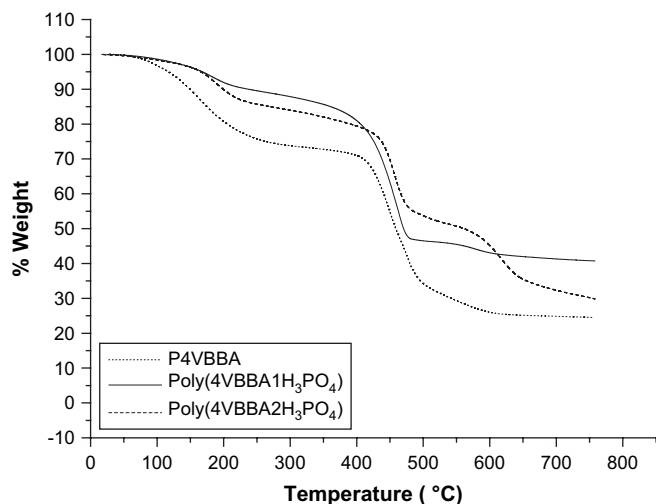


Fig. 3. TG thermograms of pure and H_3PO_4 doped P4VBBA recorded at a heating rate of $10\text{ }^\circ\text{C}/\text{min}$ under a nitrogen atmosphere.

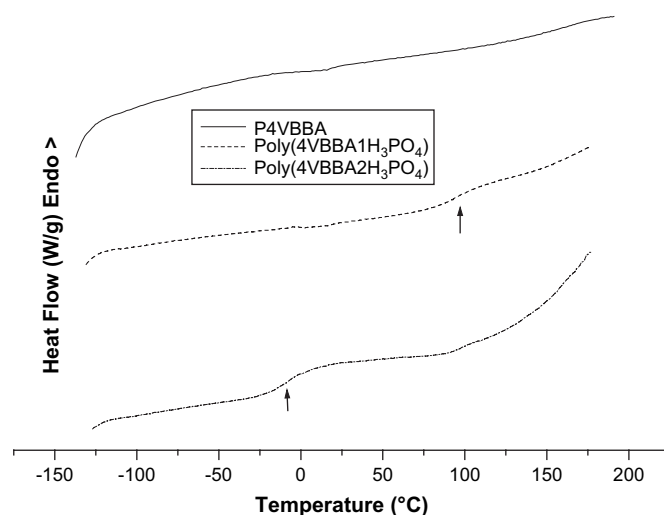


Fig. 4. DSC traces of the pure and doped P4VBBA recorded in an inert atmosphere at a heating rate of $10\text{ }^\circ\text{C}/\text{min}$.

3.3. Conductivity measurement

The alternating current (AC) conductivities, $\sigma_{ac}(\omega)$ of the polymers were measured at several temperatures using impedance spectroscopy. The frequency dependent AC conductivities ($\sigma_{ac}(\omega)$) were measured using Eq. (1);

$$\sigma'(\omega) = \sigma_{ac}(\omega) = \varepsilon''(\omega)\omega\varepsilon_0 \quad (1)$$

where $\sigma'(\omega)$ is the real part of conductivity, $\omega = 2\pi f$ is the angular frequency, ε_0 is the vacuum permittivity ($\varepsilon_0 = 8.852 \times 10^{-14}\text{ F/cm}$), and ε'' is the imaginary part of complex dielectric permittivity (ε^*). Fig. 5 displays the AC conductivity of $\text{P4VBBA} \cdot 1\text{H}_3\text{PO}_4$. The curves comprise frequency-independent plateau regions when the frequency is higher than 10^4 Hz . The DC conductivity (σ_{dc}) of the samples was derived from the plateaus of $\log \sigma_{ac}$ vs. $\log f$ by linear fitting of the data. Identical values were derived from Cole–Cole plots (Z'' vs. Z'). The irregularities at low frequency ($f < 10^4$) region are due to the blocking electrode polarizations.

The direct current (DC) conductivities of the phosphoric acid doped samples are compared in Fig. 6. The conductivity isotherm illustrates that the DC conductivity depends on doping ratio as well as the temperature. Generally, phosphoric acid doped systems exhibit Arrhenius behavior at lower acid contents and VTF behavior at

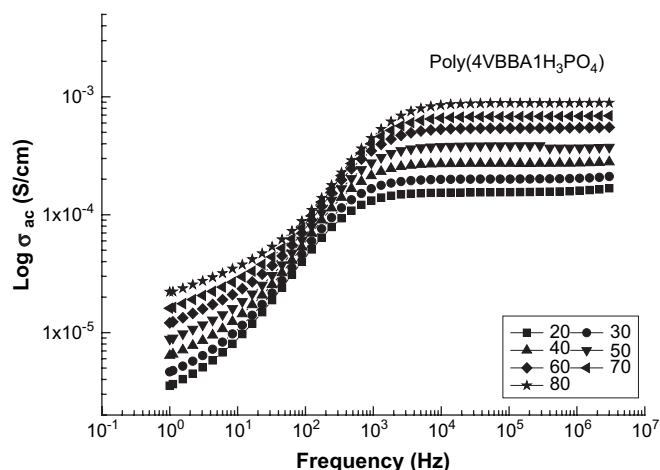


Fig. 5. AC conductivity vs. frequency (Hz) for $\text{P4VBBA} \cdot 1\text{H}_3\text{PO}_4$ at various temperatures.

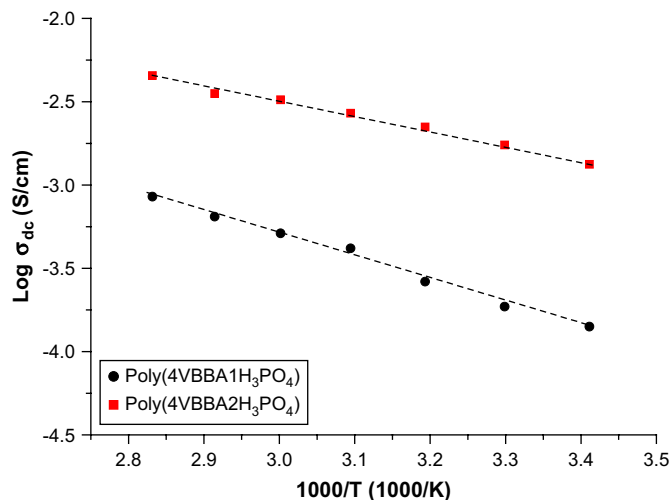


Fig. 6. DC conductivities of the P4VBBA·xH₃PO₄ as a function of reciprocal temperature.

higher acid ratio x . For P4VBBA·2H₃PO₄ (Fig. 6), the conductivity isotherm can be fitted by Arrhenius equation (Eq. (2)).

$$\ln \sigma = \ln \sigma_0 - E_a/kT \quad (2)$$

where σ_0 is the pre-exponential terms, E_a is the activation energy, and k is the Boltzmann constant. The activation energies of P4VBBA·1H₃PO₄ and P4VBBA·2H₃PO₄ are 0.27 kJ/mol and 0.175 kJ/mol, respectively.

The proton conduction in P4VBBA·xH₃PO₄ membranes strongly depends on the acid composition. However, the conductivity of the samples changes slightly with the temperature which is different from the acid doped proton conducting membranes. The proton conductivity of these homogeneous systems ranges from 10⁻⁶ S/cm to 10⁻⁴ S/cm at ambient temperature and the conductivity isotherms were described by Vogel–Tamman–Fulcher (VTF) relation [4,11]. The proton conductivity in P4VBBA·xH₃PO₄ can be explained by the absence of contribution from the host matrix where the proton diffusion can occur over the phosphoric acid phase. Similar behavior was reported for Nafion/H₃PO₄ system where the proton conductivity was approximately 0.0025 S/cm (at 100 °C) in the dry state and increased with increasing water content [16]. However, P4VBBA·2H₃PO₄ has higher proton conductivity of 0.0013 S/cm at RT and 0.005 S/cm at 80 °C under anhydrous conditions.

3.4. Solid-state NMR studies

Fig. 7 displays the one-dimensional ¹¹B 3Q-filtered MAS NMR spectra of pure P4VBBA polymer and its acid doped derivatives with two different acid concentrations. The 3Q-filtered experiment was chosen instead of direct excitation to eliminate the boron background signal from NMR probe, which leads to a strong baseline distortion. However, this method has the disadvantage of being not entirely quantitative. In pure P4VBBA, three and four-coordinated boron sites are clearly separated. The four-coordinated boron sites (ring C–BO₃) usually appear close to ~0 ppm and three coordinated boron sites (ring C–BO₂) appear at higher chemical shift values [29,30]. Moreover, the three coordinated boron sites appear as broader resonances due to their higher quadrupolar coupling as compared to four-coordinated boron sites [31–33]. Since P4VBBA system is a polymer system the boron chemical shift values can differ from those as compared to boron containing oxides [34,35]. However, shift differences due to major structural features, like the coordination of the boron sites, are expected to be

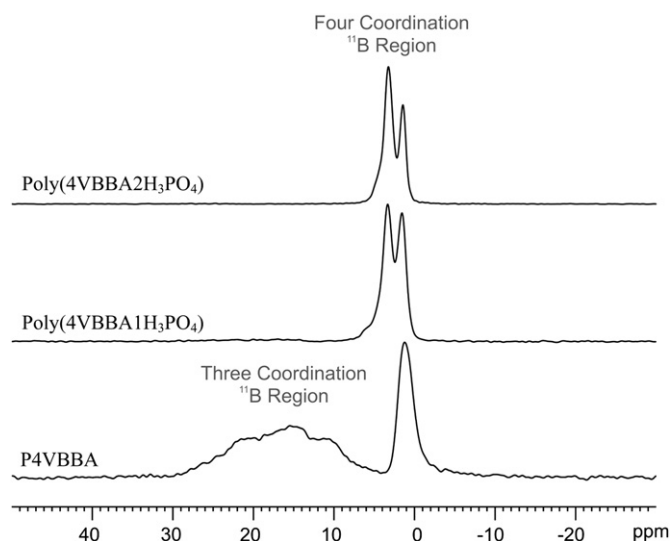


Fig. 7. One-dimensional ¹¹B 3Q-filtered MAS NMR spectra of the pure P4VBBA and its acid doped derivatives. The spectra were recorded at room temperature under 20 kHz of MAS.

similar. The sharp resonance appearing at 1.3 ppm is due to one four-coordinated boron site, and the resonance covering the chemical shift ranges from 10 ppm up to 25 ppm, is due to at least one three coordinated boron site. It is likely that more than one site is covered underneath the broad resonance, however, the number of different sites is not easy to identify from a one-dimensional 3Q-filtered ¹¹B MAS NMR spectrum. Nevertheless, the three and four-coordinated boron sites can be distinguished. In the acid doped materials, two resonances due to different four-coordinated boron sites are observed at 1.6 ppm and 3.4 ppm for the material with the lower and at 1.5 ppm and 3.3 ppm for that with the higher acid content. The broad resonance of the three coordinated boron sites is strongly reduced in intensity and thus hardly observed in the acid doped materials. This may suggest that acid doping favors or leads to a four-coordinated boron arrangement, however, changes in the local dynamics occurring upon acid doping might have a same effect. Ongoing ¹¹B NMR studies are performed in our lab to elucidate the actual number of three coordinated sites as well as the origin of their substantial loss in intensity in the 3Q-filtered ¹¹B MAS NMR spectrum after acid doping.

The effect of acid doping in the P4VBBA system is twofold. First, doping changes the ratio of the three to four-coordinated boron sites in a yet unclear mechanism, which results in an increase of four-coordinated boron sites. Secondly, the number of the four-coordinated boron site changes from one site to two sites in the acid doped materials. Moreover, the intensity ratio for the four-coordinated boron sites is changing with the amount of acid in the doped P4VBBA, in which the intensity of the high-field resonance at ~1.5 ppm is decreasing relative to the low-field resonance at ~3.3 ppm with increasing acid strength.

In Fig. 8, the ³¹P MAS spectra of the acid doped P4VBBA materials are shown. Four distinct phosphorous sites are observed at 0.2 ppm, -7 ppm, -14 ppm, and -17 ppm. The chemical shift value of ~0 ppm is characteristic for free phosphoric acid, which is present in the polymer matrix and increases the proton conductivity. The resonance at approximately -7 ppm is assigned to anhydride formation between two phosphoric acid molecules [36], which can still contribute to the conductivity via the vehicle mechanism. The other signals appearing at lower chemical shift values are most likely due to the possible anhydride formation between phosphoric acid molecules and boron sites (B–O–P

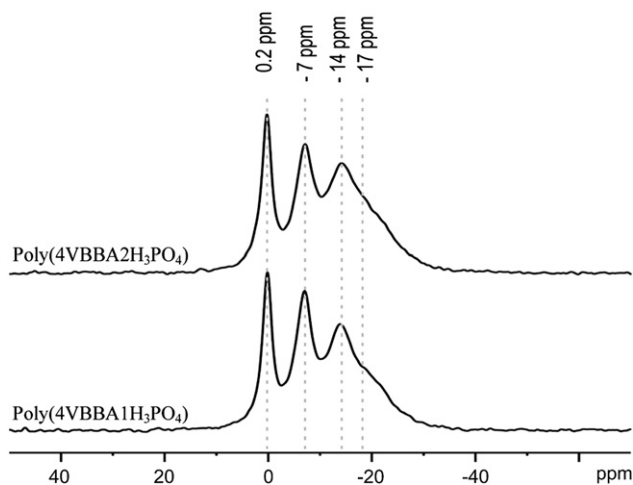


Fig. 8. ^{31}P MAS spectra of doped P4VBBA derivatives recorded at room temperature under 20 kHz MAS. The chemical shift values of the four resonances observed are given on top of the spectra.

arrangements) [21,37]. The formation of similar chemical structures has been studied before, in particular in the case of boron–phosphate glasses, where high-field shifts of 10–20 ppm of ^{31}P sites involved in the B–O–P links have been observed [40].

The assignment of the ^{31}P signals to mobile phosphoric acid sites (0.2 ppm and -7 ppm) and matrix coordinated B–O–P ^{31}P sites (-14 ppm and -17 ppm) is suggested by the line width of the NMR signals. Moreover, it is supported by ^1H – ^{31}P CP-MAS spectra (not shown), where the low field signals at 0.2 ppm and -7 ppm are strongly suppressed. The high molecular mobility of these sites, which leads to an efficient line narrowing via averaging of heterogeneities in chemical shift, causes a substantial reduction of the hetero-nuclear dipolar couplings and thus reduces the ^1H – ^{31}P cross-polarization efficiency. The high-field signals (-14 ppm and -17 ppm) are nearly unchanged, due to the immobilization of the free acid sites by linkage to polymer backbone through ^{11}B .

Relative amounts of the different phosphorous sites were determined by iterative fitting with the DMFIT program package [38] and the results are shown in Table 1. The resonance at approximately -17 ppm is much broader as compared to the former three resonances. Moreover, the increasing amount of acid in the polymer does not change the intensity ratio of the resonances significantly, which is an indication of a nearly equal distribution of the added acid between the four different phosphorous sites (free and coordinated ones).

Table 1
 ^{31}P sites of the doped P4VBBA materials and their relative amounts

Materials	Chemical shift values			
	~ 0 ppm	-7 ppm	-14 ppm	-17 ppm
P4VBBA·1H ₃ PO ₄	22%	30.5%	17%	30.5%
P4VBBA·2H ₃ PO ₄	22%	26%	16%	36%

4. Conclusions

In this work boron containing host matrix poly(4-vinylbenzylboronic acid), P4VBBA was synthesized through free-radical homopolymerization of 4-Vinylbenzeneboronic acid. Then proton conducting composite membranes, P4VBBA· $x\text{H}_3\text{PO}_4$, were produced after doping of phosphoric acid at different molar compositions

($x = 1$ and $x = 2$) with respect to the polymer repeat unit. The materials were characterized by NMR and FT-IR studies. TGA measurements demonstrated that the composite materials show almost no weight loss up to 140 °C. The exponential weight change within 160–350 °C can be attributed to intermolecular condensation of acidic units and then the materials decompose. The attachment of phosphoric acid to the polymer matrix through boron functional groups (possibly in the form of B–O–P and/or B–O–P–O–B) was confirmed by ^{31}P MAS spectra of the doped materials. Different types of three and four-coordinated boron sites exist at the same time in the un-doped P4VBBA polymer (B–OH and B–O–B) as demonstrated by ^{11}B MAS NMR. In the doped P4VBBA, however, only two different four-coordinated boron sites exist, and their ratio depends on the acid content. The addition of phosphoric acid softened the materials shifting the T_g to lower temperatures. The proton conductivity of the materials strongly depends on the acid composition reaching to 0.005 S/cm at 80 °C in dry state. The proton transport can be expected to occur predominantly by the Grotthuss mechanism via the phosphoric acid molecules. From these results it can be concluded that proton conducting acid doped P4VBBA materials can be interesting for fuel cell application since condensation reaction between boric acid and phosphoric acid form B–O–P linkages which may inhibit acid exclusion during fuel cell operation.

Acknowledgements

Support from TÜBİTAK under contract number 105M345 is acknowledged. This work was partially supported by the BMBF under the contract number GIN-SF-049. MRH acknowledges financial support by the Carlsberg Foundation.

References

- [1] Przyłuski J, Wieczorek W. Synth Met 1991;45:323–33.
- [2] Lassegues JC. In: Colombari P, editor. Solids membranes, and gels-materials and gels-materials and devices. Cambridge: Cambridge University Press; 1992. p. 311–28.
- [3] Lassegues J, Grondin J, Hernandez M, Maree B. Solid State Ionics 2001;145:37–45.
- [4] Schuster MFH, Meyer WH. Annu Rev Mater Res 2003;33:233–61.
- [5] Dippel T, Kreuer KD, Lassegues JD, Rodriguez D. Solid State Ionics 1993;61:41–6.
- [6] Donoso P, Gorecki W, Berthier C, Defendini F, Poincignon C, Armand MB. Solid State Ionics 1988;28/30:969–74.
- [7] Petty-Week S, Zupancic JJ, Swedo JR. Solid State Ionics 1988;31:117–25.
- [8] Daniel MF, Desbat B, Cruege F, Trinquet O, Lassegues JC. Solid State Ionics 1988;28:637–41.
- [9] Tanaka R, Yamamoto H, Shono A, Kubo K, Sakurai M. Electrochim Acta 2000;45:1385–9.
- [10] Rodriguez D, Jegat C, Trinquet O, Grondin J, Lassegues JC. Solid State Ionics 1993;61:195–202.
- [11] Bozkurt A, Meyer WH. J Polym Sci Part B Polym Phys 2001;39:1987–94.
- [12] Samms SR, Wasmus S, Savinell Rf. J Electrochem Soc 1996;143:1225–32.
- [13] Li QF, He RH, Gao JH, Jensen JO, Bjerrum NJ. J Electrochem Soc 2003;150:A1599–605.
- [14] Pu H, Meyer WH, Wegner G. J Polym Sci Part B Polym Phys 2002;40:663–9.
- [15] Zhai Y, Zhang H, Zhang Y, Xing D. J Power Sources 2007;169:259–64.
- [16] Savinell R, Yeager E, Tryk D, Landau U, Wainright J, Weng D, et al. J Electrochem Soc 1994;141:L46–51.
- [17] Martin C, Hunt BJ, Ebdon JR, Ronda JC, Cadiz V. React Funct Polym 2006;66:1047–54.
- [18] Moffat BJ, Neeleman JF. J Catal 1973;31:274–7.
- [19] Krishnan P, Park JS, Kim CS. J Membr Sci 2006;279:220–9.
- [20] Moffat JB, Chao EE, Nott B. J Colloid Interface Sci 1978;67:240–6.
- [21] Mikhailenko SD, Zaidi J, Kaliaguine S. J Chem Soc Faraday Trans 1998;94:1613–8.
- [22] Massiot D, Touzo B, Trumeau D, Coutures JP, Viret J, Florian P, et al. Solid State Nucl Magn Reson 1996;6:73–83.
- [23] Kahraman G, Beşkardeş O, Rzaev ZMO, Pişkin E. Polymer 2004;45:5813–28.
- [24] Şenel M, Bozkurt A, Baykal A. Ionics 2007;13:263–6.
- [25] Amoureux JP, Fernandez C, Steuernagel S. J Magn Reson Ser A 1996;123–126:116–20.

- [26] Bouchet R, Siebert E. *Solid State Ionics* 1999;118:287–99.
- [27] Zaidi SMJ. *Electrochim Acta* 2005;50:4771–7.
- [28] Baykal A, Kızılyalı M, Gözel G, Kniep R. *Cryst Res Technol* 2000;35:247–54.
- [29] Chen L, Zhang M, Yue Y, Ye C, Deng F. *Microporous Mesoporous Mater* 2004;76:151–6.
- [30] Dusterer MZ, Montagne L, Palavit G, Jager C. *Solid State Nucl Magn Reson* 2005;27:65–76.
- [31] Kroeker S, Stebbins JF. *Inorg Chem* 2000;40:6239–46.
- [32] Hansen MR, Vosegaard T, Jakobsen HJ, Skibsted J. *J Phys Chem A* 2004;108:586–94.
- [33] Elbers S, Strojek W, Koudelka L, Eckert H. *Solid State Nucl Magn Reson* 2005;27:65–76.
- [34] Lemarchand E, Schott J, Gaillardet J. *Geochim Cosmochim Acta* 2005;69:3519–33.
- [35] Schmitt-Kopplin P, Hertkorn N, Garrison AW, Freitag D, Kettrup A. *Anal Chem* 1998;70:3798–808.
- [36] So YH, Heeschen JP. *J Org Chem* 1997;62(11):3552–61.
- [37] Strojek W, Miriam Fehse C, Eckert H, Ewald B, Kniep R. *Solid State Nucl Magn Reson* 2007;32:89–98.
- [38] Massiot D, Fayon F, Capron M, King I, Le Calvé S, Alonso B, et al. *Magn Reson Chem* 2002;40:70–6.
- [39] Schmidt M, Ewald B, Prots Y, Cardoso-Gil R, Armbrüster M, Loa I, et al. *Z Anorg Allg Chem* 2004;630(5):655–62.
- [40] Zielniok D, Cramer C, Eckert H. *Chem Mater* 2007;19:3162–70.